4D Respiratory Motion-Corrected Rb-82 Myocardial Perfusion PET Image Reconstruction

Arman Rahmim, *Member, IEEE,* Jing Tang, *Member, IEEE,* M. R. Ay, *Member, IEEE,* and F. M. Bengel

***Abstract*–Routine clinical myocardial perfusion (MP) PET imaging involves the use of cardiac gating only. Nonetheless, respiratory motion of the heart can considerably degrade the quality of MP images and the quantitative accuracy of myocardial uptake estimates. We first performed a quantitative evaluation of the degrading contributions of cardiac (C) and respiratory (R) motion, as well as non-motion factors of Rb-82 positron range, photon non-collinearity, crystal scattering and penetration. For a normal human simulated phantom, we showed that the combination of all above factors resulted in ~48% underestimation of myocardial activity, while corrections for all non-motion factors resulted in 21%, 36% and 41% underestimated myocardial activities in the presence of C, R and C&R motion. This means that compensation for respiratory motion must be considered as critical towards achieving overall motion compensation and/or resolution modeling.**

To achieve respiratory motion compensation, we used translation motion vectors to first match respiratory-only gated images to the end-expiration reference frame. Next, for each cardiac gate, a 4D EM reconstruction algorithm was applied to the R-gated data within that cardiac phase. Three techniques were compared involving reconstructions of (a) a single R-gate only, and all R-gates (b) without and (c) with respiratory motion correction (MC). Using simulated PET data, quantitative comparisons of noise vs. bias trace-off curves indicated notable improvements for the proposed 4D respiratory MC method. Using CHO analysis as applied to the task of perfusion defect detection, ROC analysis of the three methods resulted in AUC values of 0.610±0.039, 0.645±0.038 and 0.821±0.029. The CLABROC statistical test revealed that the proposed MC technique significantly outperformed the other two methods in the task of defect detection.

I. Introduction

Myocardial perfusion (MP) emission computed tomography imaging allows feasible and noninvasive assessment of cardiac function and regional blood flow [1-6]. MP PET imaging is increasingly utilized because it provides improved diagnostic quality, certainty, and accuracy over conventional MP SPECT imaging [4, 7-9]. The prognostic value in predicting adverse cardiac outcomes has also been demonstrated in an increasing number of studies [10-12]. In Rb-82 PET imaging, the short half-life of the tracer (76 s) makes possible rapid MP rest/stress paired studies within a very short time, allowing rest and stress imaging under virtually identical conditions and decreasing the total time required to scan each patient. As such, cardiac PET with Rb-82 allows a readily feasible and convenient assessment of myocardial perfusion [13-19].

Cardiac and respiratory movements may introduce notable degradations in image quality, and a number of approaches have been presented in the literature to tackle these issues (e.g. as reviewed in [20]). In addition, these effects pose additional layers of challenge to resolution modeled (RM) image reconstruction efforts (i.e. techniques which attempt to characterize and incorporate additional processes responsible for resolution degradation including positron range, photon non-collinearity, inter-crystal scattering and penetration [21]).

Table 1: Effect of resolution degrading factors as well as cardiac and/or respiratory gating (8 gates each) on measured myocardial activity. Simulations were performed for the 4D NCAT phantom (normal male). The first entry (-3.2%) indicates minimal effect of motion *within* the gated frame (reference gate: end-diastole).

Gating	Motion Contam.	No Resolution Degrad.	Rb-82 Positron Range	Other Degrading Factors	Combined Degrading Factors
C&R-Gated	Within-gate	-3.2%	-23.3%	-18.6%	-31.6%
R-Gated	Cardiac	**-21.4%**	-32.9%	-30.0%	-37.8%
C-Gated	Resp.	**-36.1%**	-43.6%	-41.2%	-46.9%
Non-Gated	C&R	**-41.4%**	-46.1%	-44.4%	**-48.3%**

To quantify the relative contribution of the various resolution degrading factors, we performed a number of simulations in the presence/absence of cardiac (C) and/or respiratory (R) gating as well as other resolution degrading effect turned on/off, with results summarized in Table 1. It is seen that the combination of all effects reduced measured myocardial activity by ~48%. Yet, even if resolution degrading factors aside from motion are accurately corrected for, one will still observe 21%, 36% and 41% underestimated myocardial activities in the presence of C, R and C&R motion, as highlighted in the table. This means that compensation for respiratory motion must be considered as critical towards achieving overall motion compensation and/or resolution modeling.

In fact, routine clinical MP PET imaging continues to utilize cardiac gating only; at the same time, respiratory motion of the heart is seen to considerably degrade quantitative estimates of myocardial uptake, and in fact

Manuscript received November 4, 2010.

A. Rahmim is with the Department of Radiology, and the Department of Electrical and Computer Engineering, Johns Hopkins University, Baltimore, MD 21205 (telephone: 410-502-8579, e-mail: arahmim1@jhmi.edu).

J. Tang is with the Division of Imaging Physics and System Analysis, Philips Healthcare, Cleveland, OH 44143.

M. R. Ay is with Research Center for Science and Technology, and the Department of Medical Physics and Biomedical Engineering, Tehran University of Medical Sciences, Tehran, Iran.

F. M. Bengel is with the Department of Radiology, Johns Hopkins University, Baltimore, MD 21205

somewhat non-intuitively, relatively more so than cardiac motion does, as seen in the table. While addition of respiratory gated imaging is plausible and attempted in the literature [22, 23], dually cardiac and respiratory-gated image generation is not routine, due to statistical image quality considerations (considerable noise amplification). The present work proposes a solution to this problem in the context of four-dimensional (4D) PET reconstruction, as detailed next. The approach continues to generate cardiac gated images, as routinely used to calculate such measures as the ejection fraction; at the same time, each cardiac gated image is obtained using count-preserved respiratory motion compensated image reconstruction.

II. Methods

Four-Dimensional (4D) PET reconstruction techniques [24] provide the ability to combine multiple data frames within a single reconstruction step, as opposed to performing multiple individual reconstruction of each data frame, thus preserving overall counts reconstructed while enhancing image quality (contrast, SNR). In the context of motion compensation, this can be achieved by initial estimation of motion vectors, followed by motion-incorporated 4D reconstruction. The present work proposes and investigates a technique that aims to compensate for respiratory motion within each cardiac-gated MP image.

Motion estimation: Heart movement caused by respiratory motion has been characterized in a number of works (e.g. see review [20]); it may be concluded that this motion (unlike cardiac motion of the heart) can be assumed as rigid at the resolution levels involved in PET image reconstruction. Analysis [25] of twenty sets of 4D respiratory gated image data from normal and abnormal humans revealed respiratory motion of the heart (as well as liver, stomach, spleen and kidneys) to involve for the most part rigid translations downward and to the interior as the diaphragm contracts during inspiration.

As a result, translation vectors were used in this work to match respiratory-gated images to a reference frame (end-expiration). Making use of the list-mode acquisition capability along with cardiac and respiratory gating information, we first generated reconstructed images of the acquired data as rebinned into respiratory-only gates, followed by respiratory motion estimation (this is a more robust approach compared to performing such motion estimation from images that are additionally cardiac gated, due to the presence of considerable noise in dually-gated images, and the fact that cardiac blurred images still depict nearly the same translations due to respiratory motion). We then used least-squares difference minimization via the BFGS Quasi-Newton method with a cubic line search procedure [26] in order to estimate the respiratory translation vectors.

Motion compensation: Next, for each given cardiac gate, a 4D EM reconstruction algorithm was applied to the respiratory-gated data within that specific cardiac phase. Given an estimated initial image estimate vector $\vec{\lambda}^k$, respiratory-gated data $\vec{y}_r$ (r=1…R) within the given cardiac gate, the system matrix P, and incorporating the estimated respiratory motion operator $M_{1\to r}$ that maps the reference R-gate 1 to any given R-gate r, the 4D motion corrected (MC) reconstruction algorithm can be written as:

$$\vec{\lambda}^{k+1} = \frac{\vec{\lambda}^k}{\sum_{r=1}^{R} M_{1\to r}^T P^T \vec{1}} \sum_{r=1}^{R} M_{1\to r}^T P^T \frac{\vec{y}_r}{P M_{1\to r} \vec{\lambda}^k} \qquad (1)$$

where multiplication and division of vectors are performed element-wise, and $\vec{1}$ is a column vector with all elements equal to 1.

III. Experiments And Results

Simulations and reconstructions: To validate our approach, time activity curves of blood pool, myocardium, and other organs, as extracted from Rb-82 PET images of 5 normal patients, were averaged and smoothed, and used to simulate a 5D NCAT phantom with both gates (8 cardiac and 5 respiratory gates) as obtained after initial blood uptake (i.e. from ~0.5min). A total duration of 5min was simulated, since our previous optimization studies have shown longer scans to not enhance MP images (for the task of defect detection) [27]. Analytic simulations were performed to simulate dually gated noise-free PET data, which were scaled to clinical count levels before 100 Poisson noise fluctuations were created. Both scenarios of defect absent and present were simulated: the perfusion defect was a transmural defect spanning 40° over the anterior-lateral region and 1.5 cm over the long-axis direction. The defect region had an activity 10% less than the normal

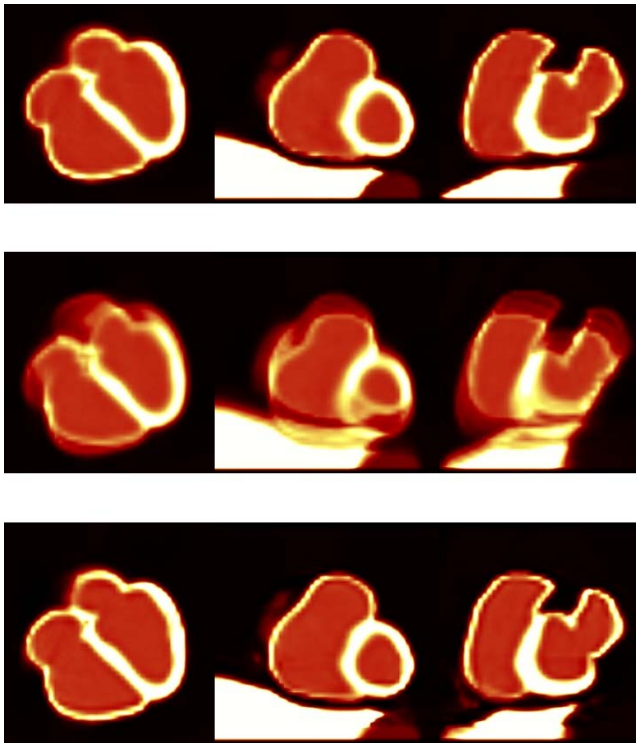

Fig. 1: Transaxial, coronal and sagittal slices of *noiseless* myocardial perfusion PET image reconstructions of the end-diastolic cardiac gate using: *(top)* end-expiration respiratory gate 1, *(middle)* respiratory-non-gated data, and *(bottom)* data processed using the proposed respiratory MC 4D reconstruction.

activity. The data were simulated for the geometry of the GE discovery RX PET/CT scanner [28], and were reconstructed using a fully validated in-house reconstruction software [21], extended to incorporate 4D respiratory MC in this work. Fig. 1 depicts sample slices of reconstructions of the end-diastolic cardiac gate using *(top)* a single R-gate (end-expiration), and all R-gates *(middle)* without and *(bottom)* with respiratory motion correction, for the noise free case. It is seen that respiratory motion significantly degrades the quality of the MP PET images, and that the proposed 4D method closely resembles the reference image at end-expiration. Fig. 2 depicts the equivalent images at clinically realistic noise levels. It is seen that the images at the top (dually cardiac and respiratory gated) are considerably noisy, while images at the middle (no respiratory gating), produce visually degraded myocardial perfusion uptake distributions in a number of areas, while the proposed 4D respiratory MC method produces qualitatively enhanced images, relative to both methods. As described next, we then performed quantitative evaluations of the resulting images.

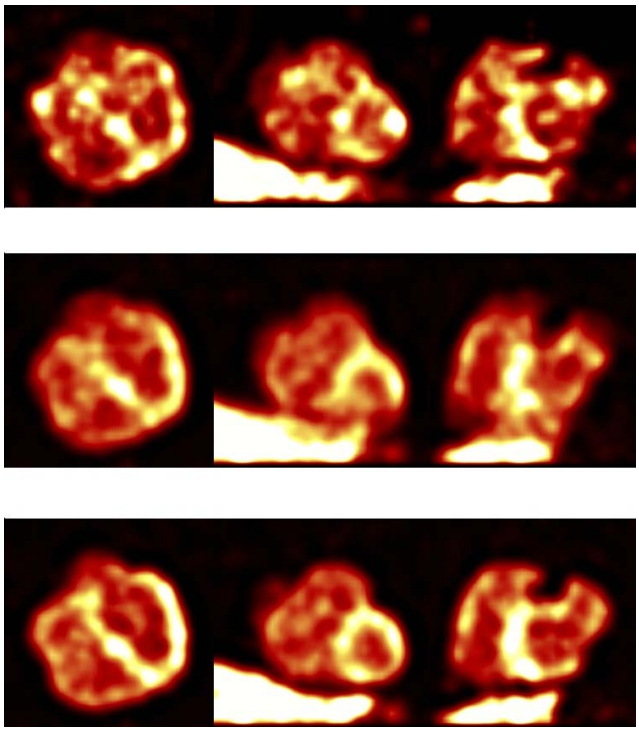

Fig. 2: Transaxial, coronal and sagittal slices of *noisy* Rb-82 MP PET image reconstructions of the end-diastolic cardiac gate using: *(top)* end-expiration respiratory gate 1, *(middle)* respiratory-non-gated data, and *(bottom)* data processed using the proposed respiratory MC 4D reconstruction.

Noise vs. Bias comparisons: As shown in Fig. 3, bias and noise levels for a given images were quantified using measures of normalized mean square error (NMSE) and normalized standard deviation (NSD), respectively. The resulting noise vs. bias curves, as generated using increasing iterations into the reconstruction, are shown in Fig. 3. The proposed respiratory MC technique is seen to clearly outperform (a) reconstruction of only one respiratory gate (expected to show degraded noise levels, but also seen to result in some bias), and (b) collective reconstruction of all respiratory gates with no MC, which was seen (Fig. 2) to exhibit resolution degraded images and therefore poorer bias performance.

ROC analysis: A channelized Hotelling observer (CHO) with four octave-wide rotationally symmetric frequency channels was applied to the reconstructed images. The start frequency and width of the first channel were both 1/64 cycles per pixel and the size of the channels was 32×32. This channel model was previously found to give good prediction of a human observer performance in myocardial defect detection [29, 30]. Each of the reconstructed images was reoriented and the short-axis slice covering the centroid voxel of the perfusion defect region was centered and cropped to the channel template size.

The resulting ratings acquired from the CHO were used to estimate ROC curves with the LABROC4 program [31, 32] as shown in Fig. 4, demonstrating improved performance with respiratory MC.

The area-under-curve (AUC) values were measured to be 0.610, 0.645 and 0.821 for reconstructions of (a) R-gate 1 only, and for collective reconstructions (b) without and (c) with respiratory MC, with respective standard deviations of 0.039, 0.038 and 0.029. The CLABROC test indicated that for the fitted ROC curves the proposed MC technique outperformed the other two methods statistically significantly with a corresponding two-tailed p-level less than 0.0001, demonstrating significant improvements in defect detection with 4D respiratory MC.

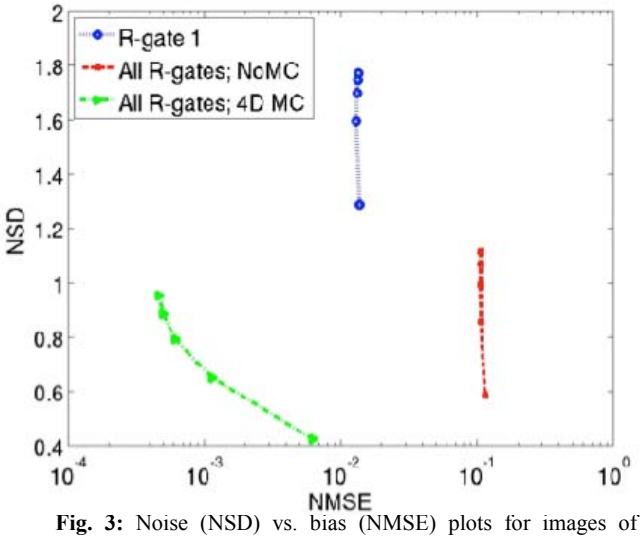

Fig. 3: Noise (NSD) vs. bias (NMSE) plots for images of cardiac gate 1 reconstructed with data from (a) only first resp. gate, and all resp. gates with (b) no MC and (c) proposed 4D MC technique.

IV. Discussion

In this work, we estimated the respiratory translation vectors

via analysis of the heart itself but applied these vectors equally to both the heart region and the liver. Without MC as additionally applied to the liver, the edge of the heart in the periphery of the liver showed considerable artifacts. In future work, we plan to investigate additional application of MC to other organs aside from the heart and the liver. Furthermore, typical respiratory movements, though seen by Segars *et al.* [25] to effectively involve only translation, were actually measured to be different for different organs: the stomach and spleen (left diaphragm) on average did not move as much as the liver (right diaphragm). The respiratory motion of the heart was also found to be less than that of the liver. As such, we plan to develop and investigate techniques that estimate and incorporate organ-specific respiratory motion vectors.

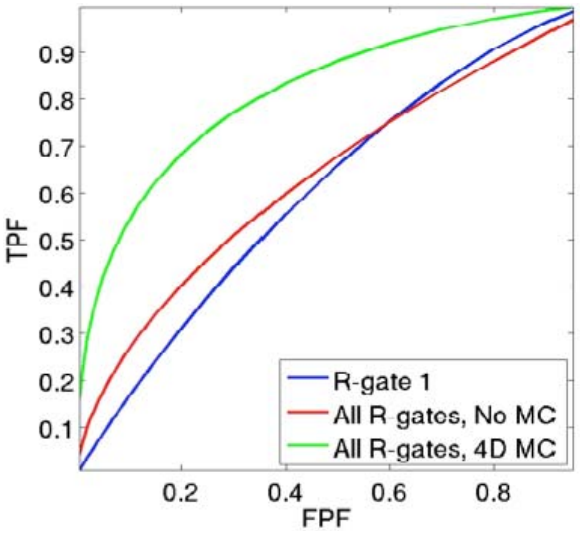

Fig. 4: ROC plots plotting true positive fraction (TPF) vs. false positive fraction (FPF) for the task of perfusion defection detection.

Furthermore, we note that Eq. (1) may need to be rendered more accurate by incorporating gate-dependent attenuation correction factors within the system matrix for each gate r [33-35]. This is a demanding problem that needs to be addressed in later work: a solution is to perform respiratory phase-matched CT (4D-CT) measurements [36, 37]; nonetheless, such an approach poses a notable increase in the effective dose, especially if performed at both rest and stress for cardiac perfusion imaging. An alternative approach we will pursue is to measure the attenuation map (using CT) at breath-hold, and to generate equivalent attenuation maps for all the respiratory gates by applying the respiratory motion vectors as estimated from the gated emission data to the reference attenuation map, as previously attempted in few respiratory-gated PET imaging applications [38-40] (though the latter works purely involved gating, and did not combine the multiple gates into a single emission image as pursued in our work).

Furthermore, we plan to perform extensive Monte Carlo simulations in order to fully validate the techniques developed in this work, as we have pursued in the past in motion compensation and image reconstruction applications [21, 27, 41-43]. Future work will also involve application of the proposed approach to Rb-82 MP PET real patient data that include both cardiac and respiratory gating information. For respiratory gating, we will utilize an infrared-camera-based motion-monitoring system (RPM System, Varian) interfaced with the GE scanner, which presently is only used in oncologic imaging. The GE toolkit 'motiontoolbox' will be used to allow generation of dually cardiac and respiratory-gated Rb-82 MP PET data.

V. Conclusions

A technique involving 4D respiratory motion-corrected image reconstruction as applied to MP PET imaging was proposed. The approach continues to generate cardiac gated images, as routinely used to calculate such measures as the ejection fraction, yet each cardiac gate additionally includes count-preserved respiratory motion compensation. The technique was seen to significantly outperform conventional imaging both qualitatively and quantitatively, including as demonstrated using noise vs. bias trade-off curves and in numerical observer defect detection.

Acknowledgment

The authors wish to thank Andrew Crabb for computational support.

References

[1] F. Dayanikli, *et al.*, "Early detection of abnormal coronary flow reserve in asymptomatic men at high risk for coronary artery disease using positron emission tomography," *Circulation,* vol. 90, pp. 808-17, Aug 1994.

[2] R. Hachamovitch and D. S. Berman, "The use of nuclear cardiology in clinical decision making," *Semin Nucl Med,* vol. 35, pp. 62-72, Jan 2005.

[3] D. L. Kraitchman, *et al.*, "Dynamic imaging of allogeneic mesenchymal stem cells trafficking to myocardial infarction," *Circulation,* vol. 112, pp. 1451-61, Sep 6 2005.

[4] J. Machac, "Cardiac positron emission tomography imaging," *Semin Nucl Med,* vol. 35, pp. 17-36, Jan 2005.

[5] L. J. Shaw and A. E. Iskandrian, "Prognostic value of gated myocardial perfusion SPECT," *J Nucl Cardiol,* vol. 11, pp. 171-85, Mar-Apr 2004.

[6] M. I. Travin and S. R. Bergmann, "Assessment of myocardial viability," *Semin Nucl Med,* vol. 35, pp. 2-16, Jan 2005.

[7] T. M. Bateman, *et al.*, "Diagnostic accuracy of rest/stress ECG-gated Rb-82 myocardial perfusion PET: comparison with ECG-gated Tc-99m sestamibi SPECT," *J Nucl Cardiol,* vol. 13, pp. 24-33, Jan-Feb 2006.

[8] U. K. Sampson, *et al.*, "Diagnostic accuracy of rubidium-82 myocardial perfusion imaging with hybrid positron emission tomography/computed tomography in the detection of coronary artery disease," *J Am Coll Cardiol,* vol. 49, pp. 1052-8, Mar 13 2007.

[9] R. E. Stewart, *et al.*, "Comparison of rubidium-82 positron emission tomography and thallium-201 SPECT imaging for detection of coronary artery disease," *Am J Cardiol,* vol. 67, pp. 1303-10, Jun 15 1991.

[10] T. H. Marwick, *et al.*, "Incremental value of rubidium-82 positron emission tomography for prognostic assessment of known or suspected coronary artery disease," *Am J Cardiol,* vol. 80, pp. 865-70, Oct 1 1997.

[11] M. P. Schenker, *et al.*, "Interrelation of coronary calcification, myocardial ischemia, and outcomes in patients with intermediate likelihood of coronary artery disease: a combined positron emission tomography/computed tomography study," *Circulation,* vol. 117, pp. 1693-700, Apr 1 2008.

[12] K. Yoshinaga, *et al.*, "What is the Prognostic Value of Myocardial Perfusion Imaging Using Rubidium-82 Positron Emission Tomography?," *J Am Coll Cardiol,* vol. 48, pp. 1029-1039, September 5, 2006 2006.
[13] E. Q. Chen, *et al.*, "Measurement of cardiac output with first-pass determination during rubidium-82 PET myocardial perfusion imaging," *Eur J Nucl Med,* vol. 23, pp. 993-6, Aug 1996.
[14] R. A. deKemp, *et al.*, "Detection of serial changes in absolute myocardial perfusion with 82Rb PET," *J Nucl Med,* vol. 41, pp. 1426-35, Aug 2000.
[15] K. Gould, "Clinical cardiac PET using generator-produced Rb-82: A review," *CardioVascular and Interventional Radiology,* vol. 12, pp. 245-251, 1989.
[16] K. L. Gould, *et al.*, "Noninvasive assessment of coronary stenoses by myocardial perfusion imaging during pharmacologic coronary vasodilation. VIII. Clinical feasibility of positron cardiac imaging without a cyclotron using generator-produced rubidium-82," *J Am Coll Cardiol,* vol. 7, pp. 775-89, Apr 1986.
[17] P. Herrero, *et al.*, "Implementation and evaluation of a two-compartment model for quantification of myocardial perfusion with rubidium-82 and positron emission tomography," *Circ Res,* vol. 70, pp. 496-507, Mar 1992.
[18] K. Knesaurek, *et al.*, "Comparison of 2-dimensional and 3-dimensional 82Rb myocardial perfusion PET imaging," *J Nucl Med,* vol. 44, pp. 1350-6, Aug 2003.
[19] J. vom Dahl, *et al.*, "Myocardial rubidium-82 tissue kinetics assessed by dynamic positron emission tomography as a marker of myocardial cell membrane integrity and viability," *Circulation,* vol. 93, pp. 238-45, Jan 15 1996.
[20] A. Rahmim, *et al.*, "Strategies for motion tracking and correction in PET.," *PET Clinics,* vol. 2, pp. *251-266*, 2007.
[21] A. Rahmim, *et al.*, "Analytic system matrix resolution modeling in PET: an application to Rb-82 cardiac imaging," *Phys Med Biol,* vol. 53, pp. 5947-65, Nov 7 2008.
[22] N. Lang, *et al.*, "Organ movement reduction in PET/CT using dual-gated list-mode acquisition," *Z Med Phys,* vol. 16, pp. 93-100, 2006.
[23] A. Martinez-Möller, *et al.*, "Dual cardiac–respiratory gated PET: implementation and results from a feasibility study," *European journal of nuclear medicine and molecular imaging,* vol. 34, pp. 1447-1454, 2007.
[24] A. Rahmim, *et al.*, "Four-dimensional (4D) image reconstruction strategies in dynamic PET: beyond conventional independent frame reconstruction," *Med Phys,* vol. 36, pp. 3654-70, Aug 2009.
[25] W. P. Segars, *et al.*, "Modeling respiratory motion variations in the 4D NCAT phantom," in *Nuclear Science Symposium Conference Record, 2007. NSS '07. IEEE*, 2007, pp. 2677-2679.
[26] D. F. Shanno, "Conditioning of Quasi-Newton Methods for Function Minimization," *Mathematics of Computing,* vol. 24, pp. 647-656, 1970.
[27] J. Tang, *et al.*, "Optimization of Rb-82 PET acquisition and reconstruction protocols for myocardial perfusion defect detection " *Phys Med Biol,* vol. 54, pp. 3161-71, 2009.
[28] B. J. Kemp, *et al.*, "NEMA NU 2-2001 performance measurements of an LYSO-based PET/CT system in 2D and 3D acquisition modes," *J Nucl Med,* vol. 47, pp. 1960-7, Dec 2006.
[29] S. D. Wollenweber, *et al.*, "Comparison of Hotelling observer models and human observers in defect detection from myocardial SPECT imaging," *IEEE Trans Nuc Sci,* vol. 46, pp. 2098-2103, 1999.
[30] S. D. Wollenweber, *et al.*, "Comparison of human and channelized Hotelling observers in myocardial defect detection in SPECT," *Journal of Nuclear Medicine,* vol. 39, p. 771A, 1998.
[31] C. E. Metz, *et al.*, "New Methods for Estimating a Binormal ROC Curve From Continuously-distributed Test Results," in *Annual Meeting of the American Statistical Association*, Anaheim, CA, 1990.
[32] C. E. Metz, *et al.*, *CLABROC*. Chicago: University of Chicago Press, 1991.
[33] F. Lamare, *et al.*, "List-mode-based reconstruction for respiratory motion correction in PET using non-rigid body transformations.," *Phys Med Biol,* vol. 52, pp. 5187-5204, 2007.
[34] F. Qiao, *et al.*, "A motion-incorporated reconstruction method for gated PET studies.," *Phys Med Biol,* vol. 51, pp. 3769-3783, 2006.
[35] T. Li, *et al.*, "Model-based image reconstruction for four-dimensional PET.," *Medical Physics,* vol. 33, pp. 1288-1298, 2006.
[36] C. C. Nagel, *et al.*, "Phased attenuation correction in respiration correlated computed tomography/positron emitted tomography," *Med Phys,* vol. 33, pp. 1840-7, Jun 2006.
[37] F. Ponisch, *et al.*, "Attenuation correction of four dimensional (4D) PET using phase-correlated 4D-computed tomography," *Phys Med Biol,* vol. 53, pp. N259-68, Jul 7 2008.
[38] H. Fayad, *et al.*, "Respiratory synchronized CT image generation from 4D PET acquisitions," in *Nuclear Science Symposium Conference Record, NSS '08. IEEE*, 2008, pp. 5488-5492.
[39] R. G. Wells, *et al.*, "Single-Phase CT Aligned to Gated PET for Respiratory Motion Correction in Cardiac PET/CT," *J Nucl Med,* vol. 51, pp. 1182-1190, August 1, 2010 2010.
[40] M. Dawood, *et al.*, "Transforming static CT in PET/CT to multiple respiratory phases," *J Nuc Med,* vol. 48, p. 41P, 2007.
[41] J. Tang, *et al.*, "Optimized regional myocardial blood flow abnormality detection in dynamic Rb-82 PET " *J. Nucl. Med.,* vol. 50 (Supplement 2), p. 467, 2009.
[42] A. Rahmim, *et al.*, "Accurate event-driven motion compensation in high-resolution PET incorporating scattered and random events," *IEEE Trans Med Imaging,* vol. 27, pp. 1018-33, Aug 2008.
[43] A. Rahmim, *et al.*, "System matrix modelling of externally tracked motion," *Nucl Med Commun,* vol. 29, pp. 574-81, Jun 2008.